Chapter

11

Ghosts in the Machine: Quality Control

11.1 Introduction

Quality **c**ontrol (QC) or **a**ssurance (QA) often raises many questions. How do you do it? Who should do it and how often? (*Do I have to do it? Can't someone else?*) Quality has become more and more a part of service provision and professional practice in radiology. QA has long been established in the imaging modalities that utilize ionizing radiation, in response to regulatory requirements. No such requirement exists for MR; nevertheless, 'best practice' dictates that quality programmes should be implemented. With all QA activity, the importance is to achieve a balance between spending too much time and resources checking everything, and getting on with clinical work. This chapter will look at the aspects best covered by a QA programme, with other elements covered in the boxes.

MR QA is largely concerned with image quality. This is normally quantified through the measurement of particular image quality parameters using specially designed phantoms or test objects (Figure 11.1). Most MR manufacturers produce their own phantoms and use them in installation and routine preventative maintenance. In this chapter we will see that:

- signal-to-noise ratio (SNR) is the most useful (and fundamental) image quality parameter and should be measured and monitored both regularly and frequently;
- at field strengths above 0.5 T SNR is fundamentally related linearly to B_0;
- geometric parameters, e.g. spatial resolution and distortion, including slice-related quantities, are essential measurements for the initial commissioning of a system or after a re-shim, and more routinely for geometry-critical clinical applications such as radiotherapy treatment planning and stereotactic surgery;
- spatial resolution is normally determined by the size of the pixels (pixel-limited), except for highly segmented sequences or where strong signal filtering is applied;
- relaxation parameters, particularly contrast and contrast-to-noise ratio (CNR) are important for protocol development and sequence evaluation;
- ghost artefacts and problems with fat saturation or water selection may give an indication of underlying technical problems with the scanner;
- national and international QA standards (AAPM, ACR, IEC, IPEM, NEMA) have been developed;
- specialized QA procedures are required for specific applications such as spectroscopy, fMRI and in clinical trials.

We will underpin this chapter with physics theory relating to SNR and resolution.

11.2 The Quality Cycle

The quality cycle for an item of radiological equipment begins with the drawing up of specifications, i.e. before purchase. On installation of a new or upgraded MR system, acceptance procedures should be carried out by an appropriately qualified MR physicist or engineer with any non-compliance receiving corrective action from the manufacturer. The acceptance report can then form the baseline for routine QA. At each point in the cycle reference to local, manufacturer or national/international standards can be made. Further details are in Box 'National and International Standards'.

National and International Standards

The National Electrical Manufacturers Association (NEMA) has published a series of standards for the methodology of image quality parameter measurement and phantom design principles. NEMA has stopped short of defining specific performance expectations or 'action criteria'. A similar approach

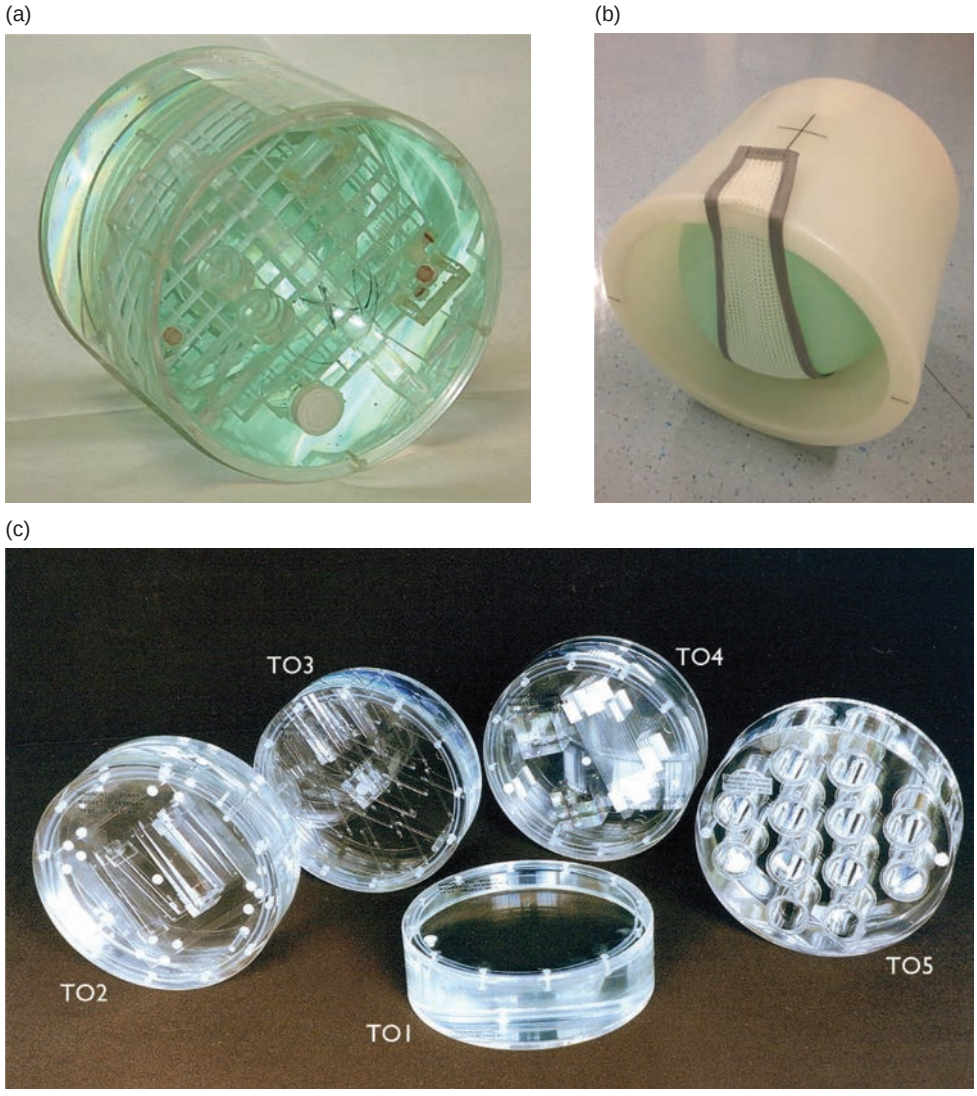

Figure 11.1 Phantoms for quality assurance (QA). (a) ACR multipurpose phantom, courtesy of the American College of Radiology. (b) Loading ring, courtesy of GE Healthcare. (c) Eurospin test object set, courtesy of Diagnostic Sonar Ltd, Livingston, UK.

has been taken by the American Association of Physicists in Medicine (AAPM) and includes action criteria. By contrast, the Eurospin Test System developed by a European Community Concerted Action programme in the 1980s is a set of five test objects for image quality evaluation, with a particular emphasis on the measurement and characterization of relaxation times (Figure 11.1c). The same group has published protocols, phantom designs and results of a multicentre trial for spectroscopic QA. The Institute of Physics and Engineering in Medicine (IPEM) has published generic and specialist (by clinical application) methodologies for quality control.

The American College of Radiology (ACR) has developed a standard for performance monitoring of MRI equipment, and its accreditation and quality control scheme uses a custom-designed phantom (Figure 11.1a) and protocol. The ACR also has defined clinical standards for performing and interpreting MRI. ACR standards include a summary of techniques, indications and contraindications, education, training and experience of personnel, staff responsibilities,

examination specifications, documentation, equipment specifications, safety guidelines, quality control and patient education. The ACR states that its standards 'are not rules but are guidelines that attempt to define principles of practice which should generally produce high-quality radiological care'.

The International Electrotechnical Commission (IEC) also has a standard for test methodologies and reporting of results in a uniform format. These standards can be found in the following publications:

American Association of Physicists in Medicine

Jackson EF, Bronskill MJ, Drost DJ, *et al.* (2010) *AAPM Report 100: Acceptance Testing and Quality Assurance Procedures for Magnetic Resonance Imaging Facilities*. College Park, MD: American Association of Physicists in Medicine.

The American College of Radiology

The ACR accreditation documents are available to download or purchase from www.acr.org/Quality-Safety/Accreditation/MRI [accessed 12 December 2014].

Of particular interest are the ACR phantoms:

www.acraccreditation.org/~/media/ACRAccreditation/Documents/MRI/LargePhantomGuidance.pdf

www.acraccreditation.org/~/media/ACRAccreditation/Documents/MRI/SmallPhantomInstructions.pdf

European Concerted Action Research Project

European Communities Research Project (COMAC BME II 2.3) (1988) 'Protocols and test objects for the assessment of MRI equipment'. *Magn Reson Imaging* 6:195–199.

European Communities Research Project (1995) 'Quality assessment in in-vivo NMR spectroscopy: results of a concerted research project for the European Economic Community I–IV'. *Magn Reson Imaging* 13: 117–158.

Institute of Physics and Engineering in Medicine (IPEM), UK

McRobbie D and Semple S (eds) (in preparation) 'Quality control and artefacts in MRI'.

International Electrotechnical Commission

International Electrotechnical Commission (2016) *Magnetic Resonance Equipment for Medical Imaging – Part 1: Determination of Essential Image Quality Parameters*. Geneva: Commission Electrotechnique Internationale.

National Electrical Manufacturers Association

The following documents can be downloaded free or purchased (all accessed 13 January 2015).

NEMA Standards, 'Determination of signal-to-noise ratio (SNR) in diagnostic magnetic resonance imaging'. Publication MS 1-2008. www.nema.org/Standards/Pages/Determination-of-Signal-to-Noise-Ratio-in-Diagnostic-Magnetic-Resonance-Imaging.aspx

NEMA Standards, 'Determination of two-dimensional geometric distortion in diagnostic magnetic resonance images'. Publication MS 2-2008. www.nema.org/Standards/Pages/Determination-of-Two-Dimensional-Geometric-Distortion-in-Diagnostic-Magnetic-Resonance-Images.aspx

NEMA Standards, 'Determination of image uniformity in diagnostic magnetic resonance images'. Publication MS 3-2008. www.nema.org/Standards/Pages/Determination-of-Image-Uniformity-in-Diagnostic-Magnetic-Resonance-Images.aspx

NEMA Standards, 'Determination of slice thickness in magnetic resonance imaging'. Publication MS5-2003. www.nema.org/Standards/Pages/Determination-of-Slice-Thickness-in-Diagnostic-Magnetic-Resonance-Imaging.aspx

NEMA Standards, 'Determination of signal-to-noise ratio and image uniformity for single-channel non-volume coils in diagnostic MR imaging'. Publication MS 6-2008. www.nema.org/Standards/Pages/Determination-of-Signal-to-Noise-Ratio-and-Image-Uniformity-for-Single-Channel-Non-Volume-Coils-in-Diagnostic-Magnetic.aspx

NEMA Standards, 'Characterisation of phased array coils for diagnostic magnetic resonance images'. Publication MS 9-2008. www.nema.org/Standards/Pages/Characterisation-of-Phased-Array-Coils-for-Diagnostic-Magnetic-Resonance-Images.aspx

NEMA Standards, 'Quantification and mapping of geometric distortion for special applications'. Publication MS 12-2006. www.nema.org/Standards/Pages/Quantification-and-Mapping-of-Geometric-Distortion-for-Special-Applications.aspx

See also 'Further reading' at the end of the chapter.

This sort of QA is concerned with equipment aspects of the scanner. Human aspects (working

practice, safety procedures, training, skill, etc.), which are much more likely to be problematical, are best addressed through clinical audit or quality management systems such as ISO 9001 or equivalent. One such scheme, organized by the American College of Radiology (ACR), consists of an initial accreditation and the development of a QA programme for all MRI facilities including the evaluation of clinical images (see Box 'National and International Standards'). All QA should be subject to audit, review and corrective action.

11.3 Signal Parameters

Signal parameters include SNR, image uniformity and centre frequency and RF transmitter gain. SNR is without doubt a key parameter. Equipment-related factors that affect SNR include field strength, choice of coil, coil loading (see Box 'Theoretical Field Dependence of SNR') and receiver bandwidth. Sequence-related factors include voxel size, sequence choice and timings. For SNR measurement it is important to use standard set-up arrangements and sequence parameters. Saving these into a user-defined QA protocol is highly recommended.

Signal parameters are normally measured using a uniform or 'flood field' phantom filled with a material with appropriate relaxation times (see Box 'Filling Factors'). A crucial issue is whether to load the coil or not. Loading means using a slightly conductive solution (i.e. saline) to mimic the reduction of the coil quality factor (see Section 10.4) and to generate realistic image noise from tissue. For head and body transmit coils a loading ring is sometimes used (see Figure 11.1b). For other coils saline can be added to the paramagnetic solution to obtain the desired effect. At 3 T, however, water-based salt solutions become problematical (see Box 'Phantom Problems').

Measurement of the centre (Larmor) frequency may also be carried out using the uniform phantom. This value is normally available through the manufacturer's prescanning software and is stored in the image series' DICOM header (see Box 'DICOM: A Common Language Leading to Misunderstanding?' in Chapter 5).

11.3.1 SNR

SNR measurements should be carried out daily or weekly. Two methods are common for measuring SNR. In the signal-background method, the signal is given by the mean pixel value from a region of interest (ROI) within the phantom. For head and body coils it is recommended that the ROI should include at least 75% of the phantom area (see Figure 11.2). The noise is measured from the standard deviation of the pixel values from small ROIs (between one and four) placed within ghost-free regions of background outside the phantom. You must take care to avoid using areas which may have atypical standard deviations, e.g. at the extreme edges of the field of view. The average of the standard deviations from these noise regions is used in the calculation of SNR

$$\mathrm{SNR} = \frac{0.66 \times \text{mean signal}}{\text{average of noise region standard deviations}}$$

The factor of 0.66 is the Rayleigh distribution correction factor and applies for a single channel coil, e.g. a birdcage coil.

The second (NEMA) method involves acquiring two identical images consecutively and subtracting them, allowing negative values in the resultant image. An ROI covering 75% of the phantom area is used to measure the signal as before. Noise is measured from the standard deviation of pixel values within this ROI placed in the subtraction image. The SNR is

$$\mathrm{SNR} = \sqrt{2} \cdot \frac{\text{mean signal in image ROI}}{\text{standard deviation in subtraction image ROI}}$$

The factor of $\sqrt{2}$ is required to compensate for the greater standard deviation from the subtraction of images. The Rayleigh correction factor is not required. Ideally, both SNR methods should yield the same result. Performance criteria are not normally quoted, being dependent upon fundamental and equipment-related factors (see Box 'Theoretical Field Dependence of SNR'). For a practical approach refer to Box 'Absolutely Fabulous SNR'. SNR is usually measured on a daily or weekly basis for either head or body coils. Other coils can be investigated less frequently on a rolling programme. This method also works for multi-element coils and when parallel imaging is used.

Filling Factors

Aqueous paramagnetic solutions such as chlorides and sulphates of nickel, copper or manganese are often used in phantoms. Alternatively, one can simply dilute leftover gadolinium contrast for a home-made phantom. It is important to understand

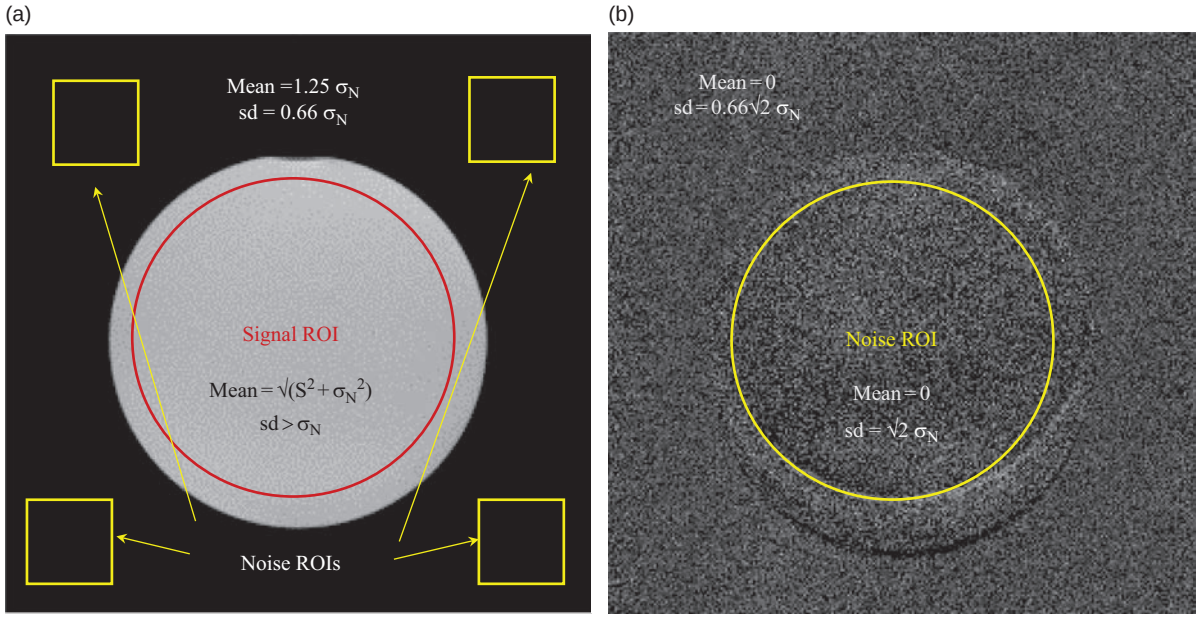

Figure 11.2 Signal-background and National Electrical Manufacturers Association (NEMA) SNR methods. (a) Magnitude image. (b) Subtraction of two consecutive magnitude images. In this example the subtraction was affected by scan-to-scan inconsistencies. σ_N is the standard deviation of the normal (Gaussian) noise distribution. S is the mean MR signal intensity of a region of interest (ROI).

the MR properties of the solution. These include the ratio of T_1 and T_2, field dependence, magnetic susceptibility and temperature coefficient, and are summarized in Table 11.1. The AAPM recommends having T_1 between 200 and 500 ms and T_2 between 150 and 300 ms. NEMA recommends only an upper limit of 1200 ms for T_1 with T_2 greater than 50 ms. We favour keeping both T_1 and T_2 quite short, e.g. both about 200 ms, as this means that the QA can be completed more quickly by using a shorter TR, and that transverse coherence artefacts can be avoided.

The relaxation time is calculated as follows:

$$\frac{1}{T_1} = \frac{1}{T_{1,0}} + R_1 C$$

where $T_{1,0}$ is the T_1 of pure water (distilled and deionized – about 3000 ms for all B_0) and C is the molar concentration of ions. For example, a 7 mM solution of $NiCl_2$ gives T_1 and T_2 approximately equal to 200 ms. The ACR phantom uses 10 mM nickel chloride plus 75 mM sodium chloride for loading, giving it a T_1 and

Table 11.1 MR properties of paramagnetic ions

Ion	T_1/T_2 ratio	Relaxivity r_1 ($s^{-1}mmol^{-1}$)		Temperature coefficient dr/dT	Comments
		3 MHz (0.07T)	60 MHz (1.4T)		
Cu^{2+}	1.1	1.7	0.5	0.038	Varies with B_0 and temperature
Gd^{3+}	1.1	22.1	10	0.28	Varies with B_0 and temperature
Mn^{2+}	2–10*	13	7		*T_1/T_2 ratio varies with B_0 but can get more 'tissue-like' T_2
Ni^{2+}	1.1	0.6	0.65	–0.006	B_0-independent up to 1.5 T; fairly independent of temperature

T_2 of approximately 150 ms at 1.5 T, but with a shorter T_2 at 3 T. However, beware of significant T_2 shortening for 3 T systems if using nickel-based solutions.

Theoretical Field Dependence of SNR

In a uniform static magnetic field of strength B_0 the equilibrium magnetization M_0 is given by the Langevin equation

$$M_0 = \frac{\gamma^2 h^2 B_0 \rho}{4 k_B T}$$

where k_B is the Boltzmann constant, T is the absolute temperature in kelvin (K), ρ is the number of nuclei per unit volume and γ is equal to 42 MHz T^{-1} for proton imaging.

The signal induced in the receive coil is proportional to the rate of change of the magnetization, i.e. the Larmor frequency ω_0, the coil sensitivity (field per unit current) B_1 and M_0 which is proportional to B_0, thus

$$S \propto \omega_0 \cdot B_1 \cdot B_0$$

Since both the Larmor frequency and M_0 are proportional to B_0, the signal (S) can be written as

$$S \propto B_1 \cdot B_0^2$$

Random noise arises from the Brownian motion of electrons within a conductor. This thermally induced random noise, sometimes called Johnson noise, is given by

$$V_{\text{noise (rms)}} = \sqrt{4 \cdot \text{kB} \cdot T \cdot R \cdot BW}$$

where R is the effective resistance and BW is the bandwidth of the measuring equipment.

The overall noise variance is the sum of the noise variances due to the patient, receive coil and receiver electronics. Effectively the resistance R is the sum of the coil resistance R_c and the resistance induced by the conductive losses in the patient R_p. Therefore $R = R_c + R_p$. In high-field imaging the dominant source of noise is the patient, whereas at low field the coil can be the dominant noise source.

If we consider the coil noise first, then we need to take account of the fact that at radiofrequencies the resistance of the coil increases with the square-root of the frequency due to the phenomenon of the skin effect. Therefore

$$V_{noise(rms)} \propto \omega_0^{1/4} \propto B_0^{1/4}$$

and for low-field systems

$$\text{SNR} \propto \frac{B_1 \cdot B_0^2}{B_0^{1/4}} \propto B_1 \cdot B_0^{7/4}$$

At low B_0 then SNR depends upon B_0 to the power of 7/4 and the coil sensitivity is crucial.

However, at high-field strengths ($\geq$0.5 T) the effective patient resistance should dominate over the coil resistance. For the simplified case of a saline sphere of radius r with conductivity σ, for a uniform B_1 field (i.e. a coil with a perfectly uniform sensitivity), R_p is given by

$$R_p = \frac{2\pi\sigma\omega_0^2 B_1^2 r^5}{15}$$

Therefore,

$$V_{noise(rms)} \propto \sqrt{B_1^2 \cdot \omega_0^2} \propto B_1 \cdot B_0$$

and

$$\text{SNR} \propto \frac{B_1 \cdot B_0^2}{B_1 \cdot B_0} \propto B_0$$

So at high-field strengths the theoretical SNR is only proportional to B_0. In practice, other factors, e.g. greater signal bandwidth and relaxation effects may reduce this dependence further. Notice that although SNR is independent of the coil sensitivity, noise and SNR are highly dependent upon the amount of tissue the coil 'sees' (proportional to the fifth power of the radius). This is the underlying reason for the greater SNR of surface and array coils.

Absolutely Fabulous SNR

The absolute SNR provides a calculation of the fundamental signal-to-noise performance of the system when measured under appropriate loading conditions and with minimal signal saturation and T_2 decay, i.e. a long enough TR and short enough TE. Absolute SNR (ASNR) can be directly related to the magnetic field strength. It is defined for conventional 2D images as

$$\text{ASNR} = \text{SNR} \frac{\sqrt{\text{pixel bandwidth}}}{\Delta x \cdot \Delta y \cdot \Delta z \sqrt{\text{NSA} \cdot N_{\text{PE}}}}$$

where the pixel bandwidth is measured in hertz and SNR is measured by any suitable method. As before, NSA is the number of signal acquisitions and N_{PE} is the phase-encode matrix size. ASNR has units of $Hz^{1/2}$ mm^{-3}. As a rule of thumb we expect ASNR to

be at least 10 $Hz^{1/2}$ mm^{-3} per tesla for an appropriately loaded head coil. So for a 1.5 T scanner with pixel dimensions of 1 mm by 1 mm and a 5 mm slice with a pixel bandwidth of 100 Hz and 256^2 matrix, expect an image SNR of $10 \times 5 \times \sqrt{256}/\sqrt{100} = 80$ $Hz^{1/2}$ mm^{-3}, assuming minimal T_1 saturation and minimal T_2 decay.

These methods can be applied to surface and special-purpose coils only with a great deal of care on the exact positioning and choice of ROI. NEMA has attempted to define a standard method for such coils. The ACR recommends measuring the 'maximum SNR' for surface coils using small ROIs for both signal and background noise.

11.3.2 Uniformity

Uniformity is particularly important for RF coils which transmit and receive, as any RF inhomogeneity will affect the flip angles and hence the contrast. Non-uniformity in receive-only surface coils is a feature of their design and is usually quite well tolerated by the observer. Homogenizing (image intensity correction) filters may be provided in the system. For this reason uniformity is usually only measured for head and body transmit coils using a uniform phantom.

Integral uniformity I is defined as

$$I = 1 - \frac{M - m}{M + m} \cdot 100\%$$

where M is the maximum pixel value and m is the minimum pixel value within an ROI of 75% of the phantom area. A value of 100% represents perfect uniformity. (NEMA uses a non-uniformity parameter $U = (1 - I)$ with a value of zero representing perfect uniformity.) To overcome inaccuracies arising from a low SNR, NEMA recommends an image smoothing stage. In practice we have found this achieves little, and for systems with low SNR it is better to increase the number of acquisitions, NSA. Performance criteria have been defined for transmit/receive head coils, and these are shown in Table 11.2. Uniformity measurements are important for accepting new coils. They can usually be incorporated with scans performed for SNR measurements. At higher field strengths (3 T and above) there is a possibility of non-uniformity arising through standing wave effects caused by the dielectric properties of water. In this

Table 11.2 Action criteria and expected performance for head coil

Parameter	ACR[a]	AAPM
SNR	Not specified	Not specified
Uniformity	≥87.5% for $B_0 < 3$ T ≥82% for $B_0 = 3$ T	≥90% for head coil up to 2 T
Linearity/distortion	±2 mm in 190 mm on diameter of phantom	≤2% over head FOV
Spatial resolution	±1 mm using ACR specified sequence	Pixel size resolved, e.g. 1 mm for 256 × 256, 256 mm FOV
Slice thickness	±0.7 mm for 5 mm slice	±10% for ≥5 mm and SE
Slice position accuracy	Bar length difference should be ≤5 mm[b] (see Figure 11.3)	±10%
Slice separation	Not defined	±10%
Low contrast object detectability	Specific to phantom Minimum ≥ 9 spokes for $B_0 < 3$ T; ≥ 37 spokes for $B_0 = 3$ T	Specific to phantom (minimum ≥9 spokes)
Ghosting	≤ 2.5%	≤1%
Centre frequency drift	Not specified	≤±1 ppm per day but expect ≤±0.25 ppm per day

[a] American College of Radiology (ACR) action criteria are dependent upon using the ACR phantom and test guidance and are somewhat stricter than those used by the ACR for accreditation, but in all cases are indicative of a minimum level of performance one can reasonably expect from a well-functioning MRI system. On the other hand, being minimum levels of performance, these criteria are not to be construed as indicators of typical or normal levels of performance.
[b] This is equivalent to an error of ±2.5 mm.

case an oil-based filling substance may be used. See Box 'Phantom Problems'.

Phantom Problems

Care has to be taken with phantom measurements to avoid obtaining misleading results. Phantoms generally contain higher signals than humans and have a different distribution of spatial frequencies, often with many high-contrast edges. The phantom geometry and materials may result in spurious susceptibility effects and the automatic shim may have trouble obtaining convergence. The filling materials may have atypical relaxation times with various consequences: greater occurrence of coherence and stimulated echoes due to long T_2, and greater high spatial frequency signals in segmented sequences. There are simple practical considerations to remember:

- allow the phantom fluid to settle;
- let the phantom fluid reach thermal equilibrium with the environment, if temperature-dependent, and check the temperature before scanning;
- avoid bubble formation;
- minimize mechanical vibration.

It's also important to remember that patients breathe, pulsate and fidget (the usual cause of image quality problems) but that phantoms do not.

For higher-field systems (e.g. 3 T) relaxation times of the test materials need to be considered. The electrical conductivity of the test object may result in non-uniform RF deposition: always use an oil phantom for uniformity measurements. Expect increased susceptibility problems: these may be related to the phantom design and construction rather than to the scanner's performance.

11.4 Geometric Parameters

Geometric parameters are mainly concerned with the accuracy of the spatial encoding, and reflect various technical factors, e.g. field uniformity, gradient linearity and eddy current compensation. Examples of specific action criteria are contained in Table 11.2. Appropriate phantoms may afford the measurement of different parameters in particular slice positions or throughout an extended volume. These are illustrated in Figure 11.3.

11.4.1 Linearity and Distortion

Linearity refers to the accuracy of distances within the image, and is usually associated with gradient amplitude calibration. Non-linearity indices L_{FE} and L_{PE} can be defined with respect to the frequency and phase axes as

$$L_{FE} = \frac{x - l}{l} \cdot 100\%$$
$$L_{PE} = \frac{y - l}{l} \cdot 100\%$$

where x is the measured distance in the frequency-encode direction, y is the measured distance in the phase direction and l is the true length in the test object. Good linearity is indicated by values close to 0%. NEMA and

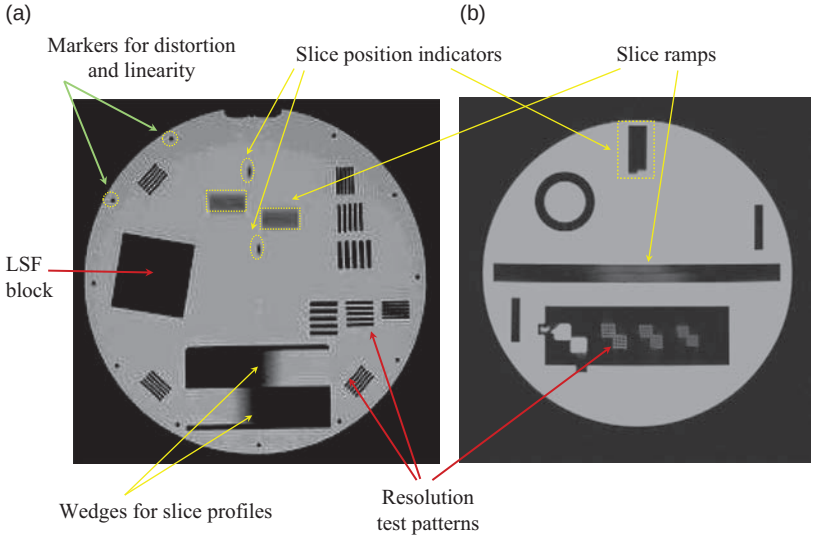

Figure 11.3 General-purpose geometric phantoms. (a) Volume phantom for which all parameters are measurable on every slice, courtesy of Charing Cross Hospital, London. (b) Slice from ACR phantom showing insert for measuring spatial resolution, slice width and slice position accuracy. LSF denotes line spread function. Courtesy of the American College of Radiology.

the AAPM do not distinguish between linearity and distortion, using similar definitions to those above (AAPM actually use the opposite, so values close to 100% mean good linearity). The ACR uses the term 'geometric accuracy'. In Europe, distortion is calculated as the standard deviation from several distance measurements, usually between an array of points spaced regularly throughout the phantom. Indices for distortion include the maximum deviation of a location from its true position or the standard deviation of the measured distances. These tests are essential at commissioning and after a field ramp or re-shim. The measurement of linearity can indicate gradient amplifier problems and is useful in routine QA. Some distortion phantom images are shown in Figure 11.4.

11.4.2 Resolution

Spatial resolution is often pixel limited in MRI, except for certain highly segmented sequences such as single-shot turbo spin echo (TSE) and echo planar imaging (EPI) and when heavy signal filtering is applied. It is therefore of minimal use in QA but may be helpful in evaluating new sequences. Quantitatively it can be assessed using bar patterns or line pairs (Figure 11.3 and Figure 11.5). These can be assessed visually or by measuring the modulation, defined (for a 100% contrast pattern) as

$$\text{modulation (line pairs)} = \frac{\text{amplitude of pattern}}{\text{mean signal across pattern}} = \frac{A}{B}$$

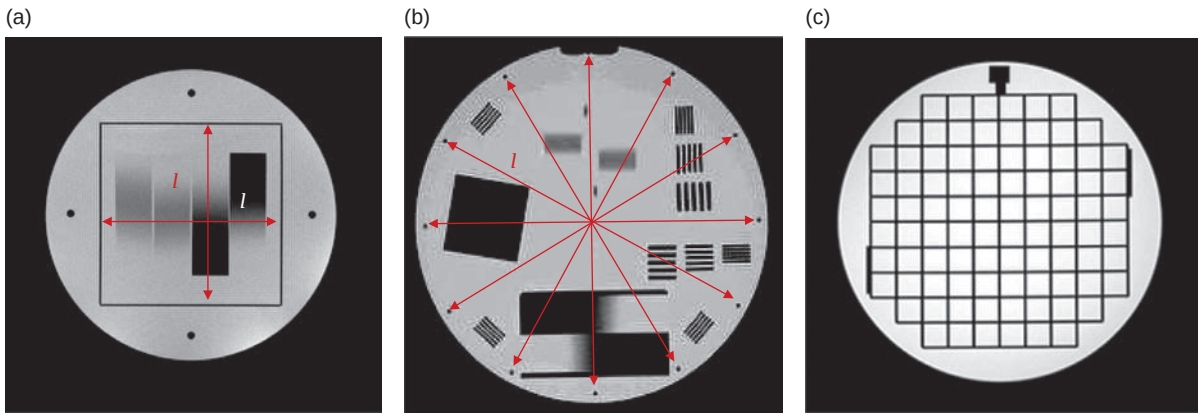

Figure 11.4 Distortion measurement phantom images. (a) Eurospin TO2, courtesy of Diagnostic Sonar Ltd, Livingston, UK. (b) Charing Cross TO2A, courtesy of Charing Cross Hospital, London. (c) ACR geometric accuracy insert, courtesy of the American College of Radiologists. *l* is the true length in the test object.

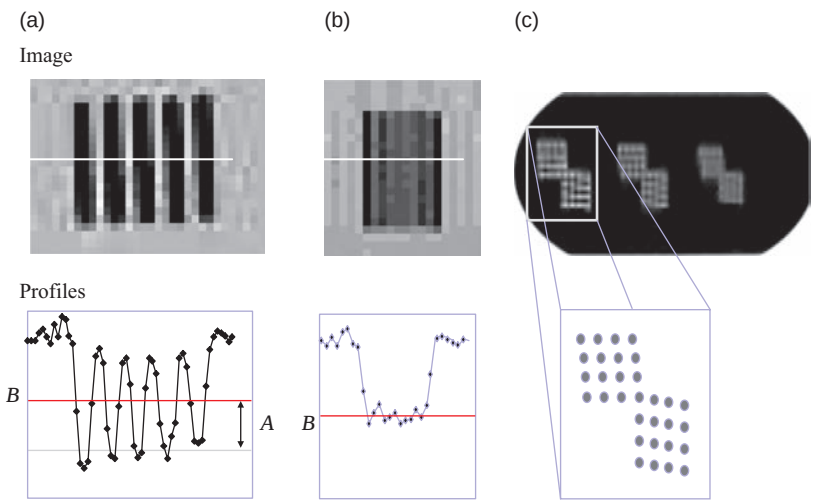

Figure 11.5 Measurement of spatial resolution from signal modulation across line pair patterns, showing (a) well-resolved and (b) poorly resolved features. *A* denotes the amplitude of modulation; *B*, the mean signal value along the profile. (c) Spatial resolution measurements from the ACR phantom using hole array pairs. Note the angular offsets of the hole array with respect to the pixel matrix. Courtesy of the American College of Radiology.

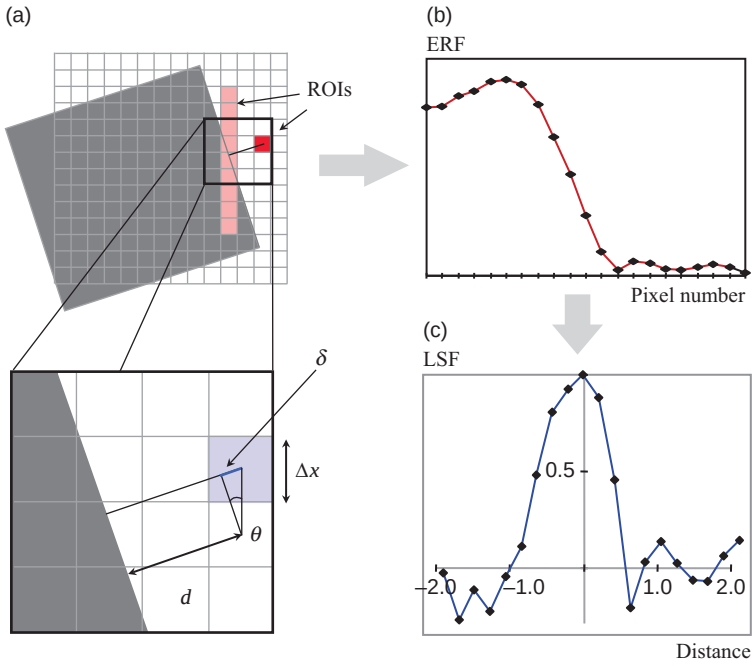

Figure 11.6 Derivation of the line spread function from an angled edge. (**a**) The edge response function (ERF) can be obtained from either a square region of interest (ROI) or a linear profile. In the latter case, the resolution measured is that perpendicular to the profile. (**b**) Example of an ERF. (**c**) The line spread function (LSF) is the normalized derivative of the ERF.

Care is required with alignment of the patterns with the pixel matrix. Aliasing of the patterns can occur and excessive Gibbs' ringing may also render the measurement void. Both effects are apparent in Figure 11.3a. More sophisticated measurements of spatial resolution are explained in Box 'Modulation Transfer Function and Line Spread Function'.

Modulation Transfer Function and Line Spread Function

In X-ray CT we would measure the modulation transfer function (MTF) of the scanner. This is not commonplace in MRI because an accurate method of MTF measurement is difficult; however, a line spread function (LSF) can be readily obtained using Judy's method. In this technique a high-contrast edge at a slight angle θ (e.g. 10°) to the pixel matrix (Figure 11.6) is scanned. For a square ROI centred on the edge, the centre of each pixel will be at a slightly different distance (as the crow flies) from the edge. The difference in distance of neighbouring pixels to the edge will be less than the pixel dimension (Δx). Hence from this ROI a magnified or oversampled edge response function (ERF) may be reconstituted. In a simpler variant of the Judy method, a line profile obliquely crossing the edge yields a similar result.

In either method the effective sampling interval is given by

$$\delta = \Delta x \times \sin\theta$$

Differentiation of the ERF produces an LSF. A measurement of the full width at half maximum (FWHM) of the LSF will give a good indication of the spatial resolution. It is vital to remember that the axis in which you are measuring the resolution is the one nearly perpendicular to the edge, i.e. the horizontal axis in Figure 11.6.

If a real-valued inversion recovery sequence (with positive and negative values) is used then it is possible to calculate the MTF as the normalized Fourier transform of the LSF. This should not be attempted for other sequences as the outer lobes of the LSF will be distorted and asymmetric and do not yield a true MTF.

An alternative method uses arrays of small holes of varying diameters. The ACR phantom (Figure 11.5c) has hole diameters of 0.9, 1.0 and 1.1 mm to allow visual assessment of spatial resolution for a nominal pixel size of 1 mm. These are slightly offset with regard to the main gradient axes to avoid aliasing problems with the pixel matrix.

Resolution Limits

The spatial resolution of an imaging method is defined as the smallest resolvable distance between two different objects. In MRI it is easy to think of the pixel size as the intrinsic spatial resolution of the image; however, this is not necessarily the case.

The pixel-limited resolution was given in Section 8.5.6. For the frequency-encode (FE) axis this was

$$\Delta x = \frac{1}{\gamma G_x M \Delta t} = \frac{1}{\gamma G_x T_{acq}}$$

where T_{acq} is the data acquisition time = $M{\cdot}\Delta t$. We could in principle increase G_x, M or Δt to achieve any desired resolution, although in practice both gradient strength and acquisition time are subject to physical limits.

The frequency spread across a pixel from the spatial-encoding gradient is

$$\Delta f = \gamma G_x \Delta x$$

However, if the signal from a point source decays over the readout period with time constant T_2^* then, following Fourier transformation, this results in the point spreading out to give a characteristic linewidth of $\Delta\omega = 2/T_2^*$, i.e. the point would be blurred by this amount. The linewidth broadened frequency Δf^* is therefore given by

$$\Delta f^* = \frac{1}{\pi T_2^*}$$

To avoid T_2^* blurring we require that

$$\Delta f \gg \Delta f^*$$

i.e.

$$G_x \gg \frac{2}{\gamma \Delta x T_2^*}$$

This also implies an ultimate limit on the spatial resolution determined by T_2^* of $2/(\gamma G_x T_2^*)$.

11.4.3 Slice Parameters

Slice parameters include slice position, slice width and slice profile (see Box 'In Profile'). Slice position can be measured from a phantom containing a pair of crossed rods or ramps inclined at θ to the slice plane (Figure 11.7). The slice position p from isocentre is then given by

$$p = \frac{d}{2\tan\theta}$$

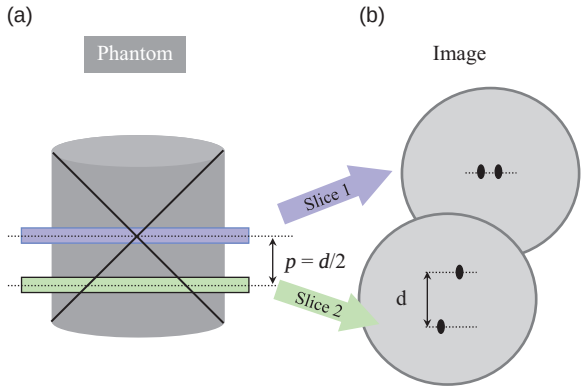

Figure 11.7 Slice position measurements from a pair of rods crossed at 45°. (a) View of phantom perpendicular to the slice-select axis showing slice positions. (b) Schematic of images produced from (a).

where d is the measured distance in the image plane. In Figure 11.7 θ is 45°. Slice separation is then the distance between adjacent slice positions.

Slice width measurements can be obtained by two methods: ramps and wedges (Figure 11.3 and Figure 11.8). Ramps may be either 'hot' or 'cold' depending upon whether they produce signal or lack of signal, e.g. a glass plate immersed in water would constitute a cold ramp. Figure 11.3 shows examples of both hot and cold ramps. The effect of the ramp is to project a magnified image or shadow of the signal in the z axis (the slice profile) onto one of the in-plane axes. A line profile drawn across this is related to the slice shape. If the ramp makes an angle θ with the slice plane the slice thickness can be determined, defined as the full width half maximum (FHWM) as

$$\text{Slice width} = \text{in}-\text{plane FWHM} \cdot \tan\theta$$

Using a different angle for the ramp or wedge changes the 'stretch factor' or degree of magnification, e.g. 26.6° gives a magnification of two while 11.3° magnifies by five. This method is adequate for slice widths down to about one-third of the ramp thickness. Below this you get an overestimation of slice thickness caused by the convolution of the ramp thickness with the slice profile (and also the in-plane pixel dimension).

Wedges can be used to measure very thin slices. An edge response function (ERF) is obtained from a line profile drawn along the wedge. The derivative of this represents the scaled slice profile, again according to the stretch factor above. This method requires a high SNR.

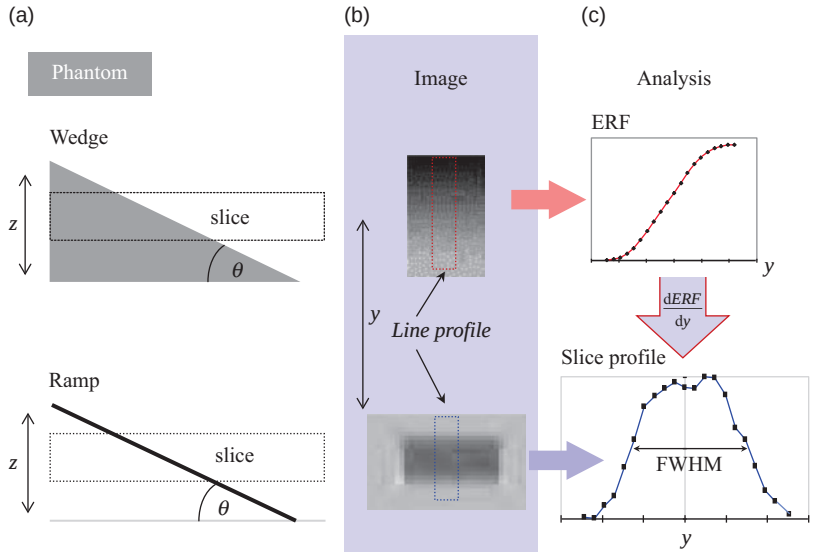

Figure 11.8 Slice width and profile measurement from a wedge and cold ramp. (**a**) View of phantom perpendicular to the slice-select axis showing slice position. (**b**) Images resulting from (**a**). (**c**) Line profiles from (**b**). ERF denotes edge response function and FWHM full width at half maximum.

In Profile

The slice profile P is a plot of the transverse magnetization (or signal) in the slice-select axis and is related to flip angle α by

$$P(z) = \rho(z) \sin \alpha(z)$$

Slice profiles are sensitive to relaxation effects, particularly T_1 when using gradient-echo sequences with short TRs. When TR/T_1 becomes less than 1, significant broadening and other distortions to the slice profile can occur in the regions where the flip angle is varying most, i.e. at the edges of the slice. These can be minimized by the use of a suitably low flip angle. For a perfectly rectangular profile, these would not occur. The need for short-duration RF pulses means that, in practice, slice profiles are never perfect. Once again, it's a case of the Fourier 'less-is-more' principle. Slice profile distortions can lead to changes in image contrast and unexpected partial volume effects (see Section 8.4).

In both methods, using pairs of opposed ramps or wedges allows one to correct for geometric misalignment with respect to the slice plane. While an exact correction is possible, it is usually sufficient to take the geometric mean of measurements across both features.

$$\text{True slice width} = \sqrt{\text{slice width 1} \cdot \text{slice width 2}}$$

Manufacturers often specify a tolerance of 10% of the slice width. These tests are important at acceptance and for sequence evaluation, especially where selective inversion pulses are used, but may not be useful in routine QA. Ramps or wedges may also be used for slice position measurements as in the ACR phantom.

11.5 Relaxation Parameters

Relaxation parameters include contrast, contrast-to-noise ratio (CNR) and T_1 and T_2 measurement accuracy and precision. Contrast is probably the most important feature of MRI; however, because it is so sequence dependent, standard QA methodologies are not common. Nevertheless contrast can be measured for pairs of samples with differing relaxation times from the mean pixel values S_1 and S_2 in ROIs placed in each sample as

$$\text{Contrast} = \frac{S_1 - S_2}{|S_1| + |S_2|}$$

where $S_1 > S_2$. The moduli on the denominator are required for inversion recovery sequences where negative signals may be encountered. This gives a contrast range of 0–1 for all sequences.

CNR may be defined as

$$\text{CNR} = \frac{S_1 - S_2}{\text{Noise}}$$

for a suitable measurement of noise (e.g. standard deviation of background).

These tests would not commonly form part of a routine QA programme, but may be very helpful in protocol optimization and for evaluating new sequences.

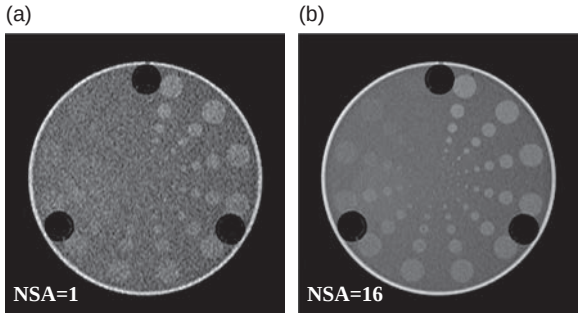

Figure 11.9 Examples of contrast-detail detectability phantom with a different number of signal acquisitions. (a) NSA = 1. (b) NSA = 16. Phantom by Philips Healthcare.

To be useful, one needs to know the appropriate relaxation times for the tissues of interest and have a suitable material that mimics them. Physical properties of tissue, such as proton density, heterogeneity, T_1/T_2 ratio, magnetization transfer and partial volumes, may not be adequately modelled by simple test materials. The Eurospin TO5 (Figure 11.1c) contains a set of doped polysaccharide gels with a range of T_1 and T_2.

Contrast-Detail Detectability

A test that is very important in X-ray-based imaging methodologies is low-contrast-detail detectability. This is a test of the resolving power of the system for low values of contrast. A typical low contrast MRI phantom is shown in Figure 11.9, where differing diameters of disk details have a different signal contrast. The image is evaluated subjectively by counting the number of disks clearly seen for each diameter group. A constructional difficulty with contrast phantoms limits this test to proton density contrast evaluation. It can also provide a subjective assessment of SNR.

11.6 Artefacts

Artefacts tend to occur sporadically and would not be subject to a routine QA test, except for ghosting.

11.6.1 Ghosting

Ghosting is best measured using a small phantom offset diagonally in the field of view (FOV). Phase ghosts will then be apparent in the phase-encode (PE) direction. Additionally, 'quadrature ghosts' (which are eliminated in modern digital receiver systems) appear as a reflection of the primary image through the origin. The fourth quadrant (Figure 11.10) should

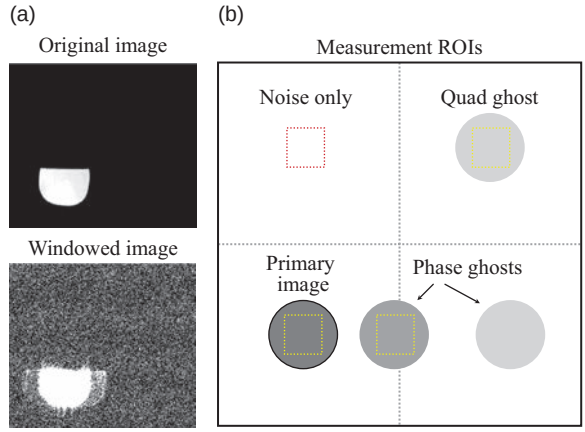

Figure 11.10 Ghosting. (a) Extreme windowing is usually required to see the ghosts. (b) Schematic diagram of ROI positions for signal–ghost ratio measurement.

contain only random noise. A **G**host-to-**S**ignal **R**atio (GSR) can be defined as

$$\text{GSR} = \frac{\text{mean SI of ghost ROI} - \text{mean SI of background ROI}}{\text{mean SI of primary image (ROI)}}$$

where SI is signal intensity. You may have to manipulate the display window and level to extreme values to visualize the ghosts, but they will always be in there somewhere. The AAPM action level is set at 1%, although we would recommend a more lenient 2% for most sequences (except EPI). Owing to the sensitivity of 2D FT to ghosting, this is a very useful test, although care needs to be taken to ensure that ghosts are not induced by mechanical vibration caused by the gradients. The presence of ghosting should be routinely investigated on a daily or weekly basis.

11.6.2 Chemical Shift and Fat Suppression

Chemical shift, as an artefact, is not worth measuring as we can determine the pixel shift if we know the receiver bandwidth (Section 7.3.1). However, it is very worthwhile to measure the effectiveness of fat suppression or water-only excitation methods as these critically depend upon the shimming of the magnet and can have a major effect upon the diagnostic value of certain examinations, especially musculoskeletal and any use of echo planar imaging (EPI).

This can be done simply using a water-based and a fat-based phantom (e.g. cooking oil) and taking the ratio of mean pixel values in images acquired with and without fat suppression enabled. The effect of

frequency-selective fat suppression on the water signal should also be tested to ensure that unwanted water signal saturation is not occurring. Care needs to be taken over shimming and the shape and positioning of the phantoms (see Box 'Phantom Problems').

11.7 Spectroscopic QA

Centres which depend heavily on spectroscopy should also perform QA regularly with an appropriate MR spectroscopy phantom which will be provided by the manufacturer. At the very least, phantom spectra should be acquired weekly using the clinical protocols (PRESS and/or STEAM at appropriate echo times; see Section 17.3). The SNR of the main peaks (creatine, N-acetyl-aspartate and choline) and ideally linewidths should be measured and recorded.

If quantification of metabolite ratios is being used regularly, a weekly check is essential. For this purpose it may be better to use a single-metabolite phantom such as N-acetyl-aspartate at a known concentration in de-ionized water. When such a phantom is made up, it must include a buffer to regulate the pH to approximately 7, and 0.1% sodium azide as a fungicide and bactericide. Peak area (i.e. absolute metabolite concentration) is extremely sensitive to RF coil characteristics, so care must be taken to ensure that the phantom can be placed in exactly the same location each time to produce the same coil loading. It is also sensitive to temperature, and if the ambient room temperature fluctuates by more than 2 °C it will be necessary to store the phantom in a fridge. In this way, although the phantom begins to warm up as soon as it is placed in the scanner, it will be at the same temperature when the MRS scan is done provided the QA is performed in the same way each time – which of course is the whole point!

11.8 Temporal Stability

In fMRI, we depend on finding very small signal changes due to neurological activity, sometimes only a 0.5% change from the resting condition. So it's extremely important that the scanner produces a stable signal from the brain tissue, over a period of at least 5 min. To be more precise, the background signal should not contain high-frequency variations; low-frequency drifts of signal intensity (SI) can be compensated during the fMRI processing steps (see Section 18.5.3).

Acquiring data to measure temporal stability is simple: just put a phantom into the head coil, and acquire using a standard fMRI protocol for at least 5 min. For a simple analysis, you can measure SI in a region of interest (ROI) on a central slice, on every volume (also known as a dynamic or a time-point). Most scanners provide ROI tools which can display SI vs time, and a quick inspection will tell you if the temporal stability is satisfactory.

For more detailed analysis, the data should be taken offline. The Biomedical Informatics Research Network (BIRN), a group of universities who collaborate on multi-centre studies, have defined a number of stability metrics to support their own work. Known as fBIRN (Functional BIRN), these metrics have become the de facto standard in the fMRI community and processing tools can be downloaded from the internet. Some vendors have incorporated these metrics into their scanner software for users. They are explained in Box 'fBIRN Processing'.

fBIRN Processing

Start by creating some new 'summary' images, using pixel-by-pixel operations on the dynamic data:

$$I_{\text{diff}} = \sum_{N=1,3,5\ldots} (I_{N+1} - I_N)$$

$$I_{\text{mean}} = \frac{1}{N}\sum_{N} I_N$$

$$I_{\text{std}} = \sqrt{\frac{1}{N}\cdot\sum_{N}(I_N - I_{\text{mean}})}$$

$$I_{\text{SFNR}} = \frac{I_{\text{mean}}}{I_{\text{std}}}$$

Using an ROI of at least 15 × 15 voxels, measure the mean μ and standard deviation σ to generate summary statistics:

$$(T)\text{SNR} = \sqrt{N}\cdot\frac{\mu_{I_{\text{diff}}}}{\sigma_{I_{\text{diff}}}}$$

$$\text{SFNR} = \mu_{I_{\text{SFNR}}}$$

For any ROI of size $n \times n$ voxels, we can define the fluctuation as

$$Fluct_n = \frac{(\sigma_{I_{\text{diff}}})_n}{\left(\mu_{I_{\text{diff}}}\right)_n}$$

and finally by taking the fluctuation at the largest ROI size and the smallest (1 × 1), we can define a measure called the 'radius of de-correlation' (RDC).

$$\text{RDC} = \frac{Fluct_n}{Fluct_1}$$

You can also measure the intensity (and temporal stability) of the EPI ghost, which is present in all images. For this, you need to make sure that the FOV of the image is at least double the size of the phantom, so that the ghost does not overlap with the main image. Measure the ghost intensity by placing an ROI around the main image, and then offset it by half the FOV in the phase-encode direction. Repeat with the offset in the opposite PE direction, so that you have two ghost ROI's at the edges of the image (Figure 11.12). Calculate the ghost level:

$$\text{Ghost}\% = \frac{SI_{\text{ghost}}}{SI_{\text{main}}} \times 100\%$$

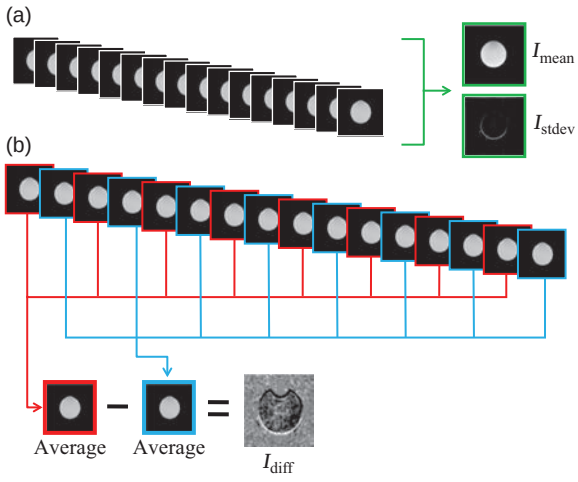

Figure 11.11 Creating summary images from fBIRN phantom scans. (a) Pixel-by-pixel, calculate the mean and standard deviation of the signal intensity (I_{mean} and I_{stdev}). (b) Calculate the mean signal intensity for all the odd-numbered time-points and even-numbered time-points, separately. Subtract the two averaged images to create the difference image, I_{diff}.

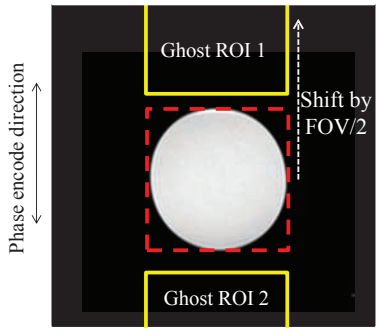

Figure 11.12 Nyquist ghost measurement in EPI (for fMRI).

Now that you have the summary metrics for your fMRI QA, how do you interpret them? Like any QA measure, they are most useful when you collect them regularly, produce a set of baseline values for your particular scanner, and then monitor for deviations. In the example shown in Figure 11.13, tracking SNR and SFNR metrics from the fBIRN analysis over a number of weeks, it is possible to detect a potential system problem. By inspecting the SI-vs-time curve for one of the later scans, sharp deviations can be seen, and it turned out that spike noise was responsible for the changes.

Some people claim that the radius of decorrelation (RDC) (see Box 'fBIRN Processing') is a measure of system 'quality' for fMRI. However, this is too simplistic. The RDC depends strongly on the basic SNR of the images. If you derive the RDC using two different head coils on the same scanner you will find that the RDC for the higher-channel coil is worse than with the simpler coil. So if you are comparing the fMRI results for two scanners, you will see that the scanner with worse SNR shows a higher RDC. That's not a good way to select the right scanner for fMRI!

Finally, there is another source of signal fluctuation in fMRI: physiological variation in the brain of the subject. Natural changes in oxygenation, caused by the respiratory and cardiac cycles, introduce changes in the fMRI signal-time curves even when the subject is not performing any task. This variation is so important that there are now many algorithms to try to remove these effects from fMRI data.

11.9 Other Specialist QA

Specialist QA may be required on a regular or per patient basis for particular quantitative, clinical investigations. Long-term stability is important for serial tumour response measurements for individual patients or in clinical trials in oncology. Geometric accuracy is paramount if MR is used for treatment planning in radiotherapy, radio-surgery or high-intensity focused ultrasound (HIFU) ablation treatment planning. It is also essential for multi-modality registration, for example with PET-CT (and hence the emergence of MR-PET – see Chapter 21). Quantitative studies of relaxation times, for example the

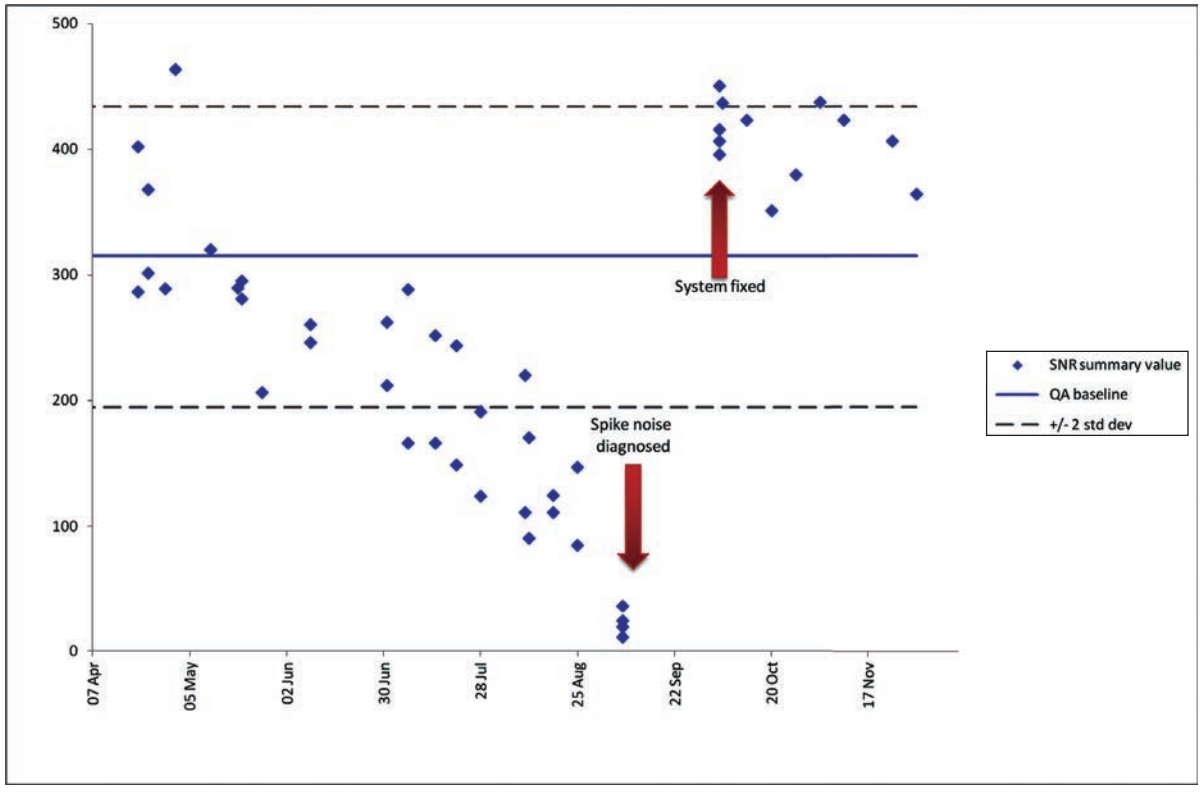

Figure 11.13 SNR tracked over several weeks using fBIRN QA procedure. During this period, the system developed a spike noise issue. By establishing the QA baseline, it is possible to distinguish between a couple of 'outliers' and the trend of decreasing performance.

assessment of organ iron overload using T_2 or T_2^* (Chapter 19), or apparent diffusion coefficient require a level of scanner and parameter precision and accuracy over and above that required for conventional diagnostic scanning.

See also:

- Image optimization: Chapter 6
- MR safety standards: Chapter 20
- Equipment-related artefacts: Chapter 7

Further Reading

ACR. www.acr.org/~/media/ACR/Documents/Accreditation/MRI/ClinicalGuide.pdf [accessed 22 March 2015].

Bodurka J, Ye F, Petridou N, Murphy K and Bandettini PA (2007) 'Mapping the MRI voxel volume in which thermal noise matches physiological noise: implications for fMRI'. *Neuroimage* 34: 542–549.

Edelstein WA, Bottomley PA and Pfeifer LM (1984) 'A signal to noise calibration procedure for NMR imaging systems'. *Med Phys* 11:180–185.

fBIRN tools: www.nitrc.org/projects/bxh_xcede_tools [accessed 2 November 2014].

Judy PF (1976) 'The line spread function and modulation transfer function of a computed tomography scanner'. *Med Phys* 3:233–236.

Lerski RA, McRobbie DW, Straughan K, *et al.* (1988) 'Multi-centre trial with protocols and prototype test objects for the assessment of MRI equipment'. *Magn Reson Imaging* 6:201–214.

McRobbie DW (1996) 'The absolute signal-to-noise ratio in MRI acceptance testing'. *Br J Radiol* 69:1045–1048.

McRobbie D and Semple S (eds) (in preparation) *Quality Control and Artefacts in MRI*. York: Institute of Physics and Engineering in Medicine. www.ipem.ac.uk.

Box 'National and International Standards' for details of ACR, IPEM and NEMA standards.